Applied Engineering
2021; 5(1): 22-34
http://www.sciencepublishinggroup.com/j/ae
doi: 10.11648/j.ae.20210501.17

Remote Monitoring of Surface Roughness on Turned and Milled Carbon Steels with High-Speed Steel and Tungsten Carbide Tools

Ludovic Ngongang[1, *], Thomas Kanaa[1, 2], Ebenezer Njeugna[1], Atangana Ateba[1]

[1]Laboratory of Mechanics, Postgraduate School for Pure and Applied Sciences, University of Douala, Douala, Cameroon

[2]Laboratory of Applied Engineering and Biotechnology, Higher Technical Teacher Training College Ebolowa, University of Yaounde I, Ebolowa, Cameroon

Email address:

ludovicngongang@gmail.com (L. Ngongang), thomas.kanaa@univ-yaounde1.cm (T. Kanaa), njeugna@yahoo.fr (E. Njeugna), aajean2003@yahoo.fr (A. Ateba)

[*]Corresponding author

To cite this article:

Ludovic Ngongang, Thomas Kanaa, Ebenezer Njeugna, Atangana Ateba. Remote Monitoring of Surface Roughness on Turned and Milled Carbon Steels with High-Speed Steel and Tungsten Carbide Tools. *Applied Engineering*. Vol. 5, No. 1, 2021, pp. 22-34.
doi: 10.11648/j.ae.20210501.17

Received: April 23, 2021; **Accepted**: May 10, 2021; **Published**: May 21, 2021

Abstract: Machinists and Metrologists are most often called to take decisions for least machining to achieve specific surface qualities of mechanical organs used in aeronautics and other severe environments. The highest challenge they face is in decision-making about the surface finish related to the cutting conditions, the tool life, and the machined material. This paper proposes a method of remote measurement and prediction of the surface roughness on turned and milled carbon steels with high-speed steel and tungsten carbide tools, based on the image acquisition protocol, material content and tool life. The remote measurement of the surface roughness involved a point-to-point viewing angle to capture the image surfaces to appreciate the ideal angle of optimal optical measurement. The assessment of the optical roughness involved the line profiling calculation method on the locally corrected pixels' values before the areal integration. The optical roughness values were regressed on the reference values and the precision of the method was assessed. The angles of 60°, 75°, and 120° show the effectiveness of the measurement method with precision attaining 83%. For the roughness prediction in the milling and turning operations with high-speed steel and tungsten carbide tools, the fuzzy logic and artificial neural networks techniques are compared considering the cutting conditions as fixed, the carbon percentage and the tool life, all as inputs. With an overall measurement precision above 90% and very low mean square errors, the qualifiedness of the predictive methods is underlined.

Keywords: Surface Roughness, Remote Monitoring, Prediction, Fuzzy Logic, Artificial Neural Networks, Machining

1. Introduction

More than a necessity, the surface becomes indispensable in almost all sectors of the industry [1-3]. Surfaces guarantee the functions of leak tightness, adhesion, solidity, resistance to wear, and corrosion, and therefore require specific attention during machining operations. More than twenty (20) factors divided into machine parameters, cutting phenomena, properties of workpiece and cutting tool, contribute to the surface finish [4]. And, coupled with productivity and efficiency reasons, the surface roughness accordingly must be mastered in terms of measurement and prediction. With regard to the high performances awaited from the machined parts in relation to their function in aggressive or precise environments [5], together with the great number of parameters defining the surface finish, important decisions have to be taken for the fast and accurate measurement and material selection. Thus, the remote measurement of the surface roughness parameters and the development of decisive predictive techniques become the essence of this mastery [6].

For decades now, the measurement of roughness parameters with the contact line profiling method remains the most widespread technique [1, 7-9] despite its limitations in terms of poor rendering of the effective surface information [1, 9-11]. This limitation is imposing the authors to remotely

assess the roughness parameters by regressing the areal optical roughness values on the contact line profiling values considered as reference [9, 12]. Furthermore, the remote estimation of roughness parameters implies some major aspects in the technology and acquisition systems of the optical evaluation techniques. When computing the optical roughness, very few authors put an emphasis on the acquisition protocol related to the focal distance, acquisition angle, light intensity, etc. [12-14]. In order to facilitate the introduction of optical techniques to the metrologists, more information needs to be given about the settings of the optical device for image acquisition of surfaces prior to the optical roughness calculation or the introduction of the images to the related softwares.

Two major directions organize the optical roughness calculation: the statistical distribution of the pixels' values on the grayscale and colour images [12, 13, 15, 16] and the estimation functions of surface texture parameters [8, 17-19]. In the first direction in respect to investigating the statistical distribution of light intensity over the image, Manjunatha et al. (2017) [16] calculated the roughness parameters by regressing on the roughness tester values, the standard deviation, and the root mean square of the pixels' values from the grayscale images. Standard deviation represents the predominant parameter regarding its correlation value. Liu Jian et al. (2017) [12] measured surface roughness with the color distribution statistical matrix (CDSM). The method deployed an analysis of the roughness correlation with the brightness variation of the red-green light on the 2D and 3D images related to their orientation on the ground specimens. The results presented a strong interrelation between roughness and brightness when the red-green light sources are vertically aligned and there was an emphasis on the placement of the machined surface signatures (striae).

The second direction apropos of texture parameters algorithms, Anayet et al. (2011) [8] generated the surface topography from the images acquired on the surface of *rubert visotactile* rugotests. A correlation factor of 0.96 permitted to validate the approach. Kamguem et al. (2013) [13] constructed the correlation function between the roughness tester values and the grey level, the average cycle, and the gradient factor of the images at 50x, 100x, and 150x magnifications. The highest correlation factor is established from the 50x magnification and the average cycle of the texture. Mateos et al. (2014) [20] designed a topographical reference of *TESA* rugotests and then determined the amplitude of the specimens prior to their correlation with the said reference. The results suggested the non-exploitation of RC and 2RC filters for the roughness tester.

The mastery of the surface finish through prediction techniques involves supervised learning methods with the roughness values from the reference measurement (using the roughness tester) to appreciate the deviation of the predicted values. In most cases, the prediction exercise reveals the cutting conditions as the most used inputs, all techniques considered. Few techniques can therefore be highlighted: fuzzy logic [3, 21-26], the artificial neural networks [27-30], the response surface methodology [5, 22, 26, 31], the genetic algorithms [31, 32] and the hybrid methods, namely, ANFIS, GA-ANN, GA-Fuzzy, and so on [32-34]. Furthermore, an emphasis on noteworthy predictive techniques of surface roughness puts the fuzzy logic and artificial neural networks at the pole position [22, 35].

In the fuzzy logic setting, together with the cutting conditions as input, some authors added the cutting fluid and the cutting tool's conditions. Kuram et al. (2013) [22] studied the roughness behavior with the use of rotational speed, feed, depth of cut, and two vegetable-based cutting fluids (one and two surfactants) as inputs on a drilled AISI 300 with HSS tool. The Taguchi's L9 orthogonal array contributed to design the fuzzy logic system whose prediction results were compared to those of the regression method. Fuzzy logic technique showed a major correlation with the input factors, all cutting fluids considered. Kovac et al. (2013) [23] applied fuzzy logic for the prediction of the surface finish in milling AISI 1060. The Mamdani inference system was implemented taking cutting speed, feed, depth of cut, and flank wear as inputs. The membership function used the Gaussian model over thirty (30) experiences and the defuzzyfication was carried out on the centroid of the area. The results portrayed a precision of 94%. Tzu-Liang et al. (2016) [26] established a new method for surface finish prediction with fuzzy set theory on milling specimens. The design of experiments technique contributed to classify the overriding factors among feed rate, cutting speed, depth of cut, nose radius, and cutting fluid. The fuzzy models designed with the first three factors generated a system with 95% of precision. Ngerntong et al. (2020) [36] predicted the surface roughness of 7075-T6 aluminum with its chip morphology in milling, using fuzzy logic. The Mamdani inference system was built around the continuation chip, the deformation chip, and the thickness chip organized in twenty (20) levels each for four (04) ranges of qualitative decision per input. The fuzzy logic technique is concluded as accurate and reliable for the surface finish prediction.

In the non-conventional machining, the fuzzy logic technique engages the cutting conditions as input with other intrinsic machining conditions. Kanish et al. (2014) [37] developed a fuzzy model to predict the improvement of the surface finish in magnetic field abrasion. The voltage, the machining gap, the rotational speed of the electromagnet, and the abrasive size were taken as inputs for the Mamdani inference system. Nine (09) rules helped in fuzzifying the system and the centroid of area was used for defuzzification. A precision of 94.6% was recorded in validating the method. Abhinav et al. (2015) [24] predicted the surface finish in electrochemical machining processes. Mamdani inference system of fuzzy model was used through eight (08) experiences taking voltage, feed, and concentration as inputs. A precision of 92.66% was recorded for the approach.

With reference to the other most used predictive technique, artificial neural networks, Vishal et al. (2008) [26] developed a neural network method to predict surface roughness with the help of the approaching angle, feed, and depth of cut. The

back-propagation training algorithm was deployed for processing the input values of the calculated number of neurons and epochs. With 76.4% of accuracy, the model presents the weakness of roughness prediction with approaching angle, speed, and depth of cut and its strength with the feed rate. Vrabel et al. (2012) [28] predicted surface finish in drilling Udimet 720. The chosen input parameters were cutting speed, feed, thrust force, and tool flank wear. Five hidden layers employed the sigmoid function as the activation function. The method achieved 87.3% of precision. Rajesh et al. (2014) [38] employed the artificial neural network to predict the surface finish with the help of speed, depth of cut, feed rate, and stepover. The sigmoid function as the transfer function and the backpropagation algorithm contributed to build and train the system. The performance of the method was assessed with sixteen (16) experiences for training and seven (07) for evaluation. A precision of 93.58% was attained in those conditions.

Kuldip et al. (2015) [34] engaged *Levenberg-Marquardt* algorithm to train the system to predict the surface roughness in turning operation from a database already built. The cutting speed, feed, and depth of cut were the input factors selected to construct the neural networks predictive function. The mean absolute percentage error over the twenty-seven (27) experiences used for the prediction was 1.7%. Vasanth et al. (2020) [30] predicted the surface roughness of the hardened SS410 steel in turning operation. The cutting force, tool wear and vibration, speed, depth of cut, and feed were taken as inputs. The sigmoidal function was used to train the 6-1-4-3-1 neural network and helped to adjust the weights of the inputs to minimize the root mean square error (RMSE). With three new inputs (cutting force, tool wear, and tool vibration), they recorded precisions above 96% related to the various combinations and subtractions of some inputs.

In sum, the measurement of surface roughness with remote techniques is barely not presented as associated with the acquisition angle of the image capture and the assessment of the optical roughness is not built around the mathematical principle used in obtaining values from the roughness tester (reference values). Likewise, concerning the prediction techniques, three to four common factors are engaged in forecasting the surface finish, over the minimum of twenty factors so far recorded.

To address the aforesaid aspects in measurement and prediction, this study aims at assessing remotely the surface roughness with an algorithm built from the mathematical principle of the roughness tester regarding the acquisition angle. In like manner to predict, with fuzzy logic and artificial neural networks, the surface finish with the tool life and the specimens' grade. Thus, in Section 2 we present the materials put in contribution to manufacture the samples as well as the methods developed for the remote monitoring and prediction of the surface roughness. In section 3, we highlight the findings.

2. Materials and Methods

2.1. Materials

The carbon steels 1010, 1015, 1020, 1035 were chosen as specimens because of their employability and the possible treatments they can undergo. Additionally, the variation of carbon percentage in the specimens helped in monitoring its impact over the surface roughness. The specimens were verified with the spectrometer Foundry Master Optik 01N0096 and the results are taken down in table 1. The late machine Comec LGA180N was used with the high-speed steel tool: HS6-5-2 (M2) and the tungsten carbide tool: PCLNR 2525-M12 with CNMG 12 04 08 carbide insert. The Milling Machine Tiger FU90 was used with the high speed steel: Shell-end milling cutter 620075, and the tungsten carbide tool: BAP400R-63-22 Face milling cutter with 4 flutes, APMT1604 PDER M4*10-T15 with M2-80 carbide inserts.

Table 1. *Average values of the chemical composition of the specimens.*

Specimen	Number of tests	%Fe	%C	%Si	%P	%S	%Cr	%Mo
1010	3	97.8	0.08	0.026	0.067	>0.3	0.02	<0.005
1015	2	98.5	0.148	0.215	0.026	0.02	0.03	0.007
1020	4	98.8	0.249	0.029	0.03	0.037	0.052	0.006
1035	3	98.4	0.421	0.165	0.026	0.301	0.044	0.007

The stopwatch Sienoc Digital Professional LCD helped for the real-time measurement of the tool life during the machining processes. The roughness tester SRT6210 contributed to measure the reference average roughness (R_{ref}). The microscope MV900 with 10X magnification was mounted on the somikon support for the acquisition process in different angles of machined surfaces. Matrix Laboratory (Matlab, student version *R2017a*) built-in platforms were used to deploy fuzzy logic and artificial neural networks prediction algorithms. The portable computer HP (Hewlett Packard) Intel© Core™ i7-8550U @1.80GHz – 1.99GHz processed the said algorithms.

2.2. Machining of Samples

The cutting conditions in turning and in milling of 1010, 1015, 1020, and 1035 steels are recorded in table 2. Leaning to the accuracy of the measurement exercise, three (03) samples were dry-machined per steel grade per machining operation following the cutting conditions (table 2).

Table 2. *Cutting conditions of specimens in turning and milling operations (V_c in m/min, DoC in mm, f_{tool} in mm) to the length of a specimen at L=28mm.*

Steel grade	Turning						Milling					
	$Ø_{spec.}$	Cutting conditions					$Ø_{cutter}$	Cutting conditions				
		V_c	f_{calc}	f_{tool}	N	DoC		V_c	fz_{calc}	fz_{tool}	N	DoC
1010	40	40	0.2	0.2	260	0.5	50	40	0.128	0.15	255	0.5
		150	0.2	0.4	1150		60	150	0.15	0.15	708	
1015	30	40	0.2	0.2	420		50	40	0.128	0.15	255	
		150	0.1	0.4	1520		60	150	0.15	0.15	708	
1025	40	40	0.2	0.2	260		50	40	0.128	0.15	255	
		150	0.2	0.4	1150		60	150	0.15	0.15	708	
1035	30	40	0.1	0.2	270		50	40	0.128	0.15	255	
		150	0.2	0.4	1520		60	150	0.15	0.15	708	

☐ HSS cutting conditions, ▨ WC cutting conditions; Ø: diameter; f_{calc} / f_{tool}: calculated/selected feed (turning).
fz_{calc} / fz_{tool}: calculated/selected feed (milling) DoC: Depth of cut N: rotational speed of the sample/tool.
V_c: Cutting speed.

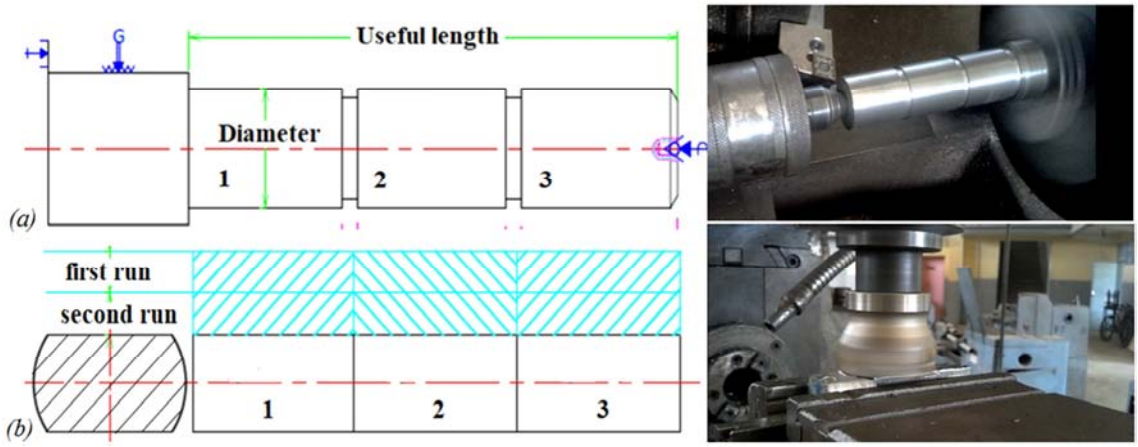

Figure 1. *Samples machining protocol: (a) in turning – (b) in milling.*

Figure 2. *Samples after the first machining operations: (a) turned specimens – (b) milled specimens.*

Two (02) runs per sample were carried out on each sample to enlarge the database (reference roughness and images) and to control the tool life (figure 1). The tool-in-cut time was recorded during machining and then calculated [15]. The samples are presented in Figure 2.

2.3. Image Acquisition Protocol

After machining, the sample surface was cleaned with compressed air and then positioned on the support coupled to the microscope. The focal distance was adjusted at 20mm above the surface. The captures were then performed at 80°, 85°, 90°, 95°, 100° in turning, and 60°, 75°, 90°, 105°, 120° in milling (figure 3).

Without regard to the acquisition angles, two (02) principal criteria organized the database of images. The first was built on a classification of images according to the nature of the cutting tool (high-speed steel and tungsten carbide) and then associated with their roughness reference values. The second was established to densify the database, thus fine-tuning the precision. And so, there was no codification of images related to the cutting tool, but still, they were linked to their roughness reference values.

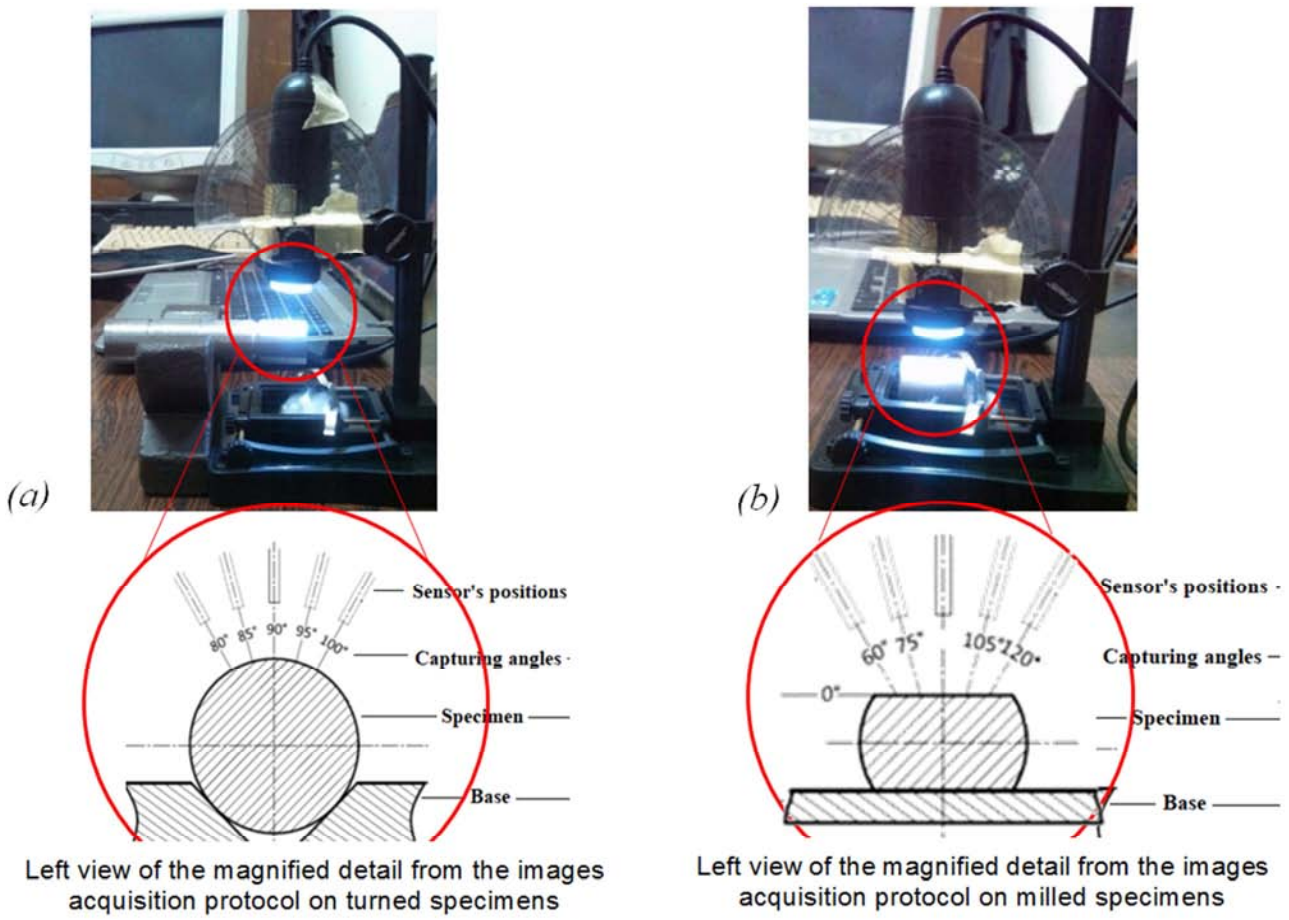

Figure 3. *Images acquisition protocol: (a) with turned specimens – (b) with milled specimens.*

2.4. Surface Roughness Measurement

The color image from the microscope is converted into grayscale. The histogram equalization is applied to improve the image contrast. The Gaussian filter is then applied to reduce the effect of the waving parameters. The optical roughness S_a has been first calculated locally S_{ar} using a 3*3 window following equation (1) and then area integrated on the whole surface with the consideration of 3 neighbours for corner pixels and 5 neighbours about end-pixels.

$$S_{ar}(i,j) = \frac{1}{9} \sum_{k=j-1}^{j+1} \sum_{l=i-1}^{i+1} I(l,k) \quad (1)$$

The remote roughness R_{rem} was a result of the regression of the optical values of the parameter S_a over the reference value R_{ref}. Following the first criterion (§2.3), forty (40) values were used to train the system and twenty (20) to evaluate. In like manner for the second, eighty (80) values were employed to train the system and forty (40) to assess it. The performance of the method was then weighed with the relative error ε.

2.5. Roughness Prediction with Fuzzy Logic and Artificial Neural Networks

Aiming at assessing the major influence of tool life and workpiece material over the surface roughness as questioned by Kanaa et al. (2016) [15], the input factors were the tool-in-cut time (Tc) and carbon percentage (%C) for both predicting methods. Tables 4 and 5 present the experiences (runs) related to the values used to train the predictive systems in turning and milling operations, respectively.

Regarding the fuzzy logic, the cutting conditions (spindle speed, feed, and depth of cut) were considered as fixed. The membership functions of the inputs were built over eight (08) subsets in the interval [0; 0.45] for the percentage of carbon (%C). Likewise, twenty-four (24) subsets in the interval [0; 2280] were built for the tool life (Tc). Table 3 presents the decision organization that helped in defining the fuzzy sets related to the study.

The inputs have been coded as X1 for the rotational speed; X2 for the feed; X3 for the depth of cut; X4 for the percentage of carbon, and X5 for the tool life and the predicted surface roughness is Y.

Table 3. *Decision table for the fuzzy logic prediction.*

Inputs	Fuzzy set appreciation	Ranges with centroïd
Rotational speed (X1) Feed (X2) Depth of cut (X3)	Very Low (VL)	
	Extra low (EL)	0 – 0.05 – 0.10
	Very low (VL)	0.05 – 0.10 – 0.15
	Low (L)	0.10 – 0.15 – 0.20
Carbon percentage (X4)	Medium (M)	0.15 – 0.20 – 0.25
	High (H)	0.20 – 0.25 – 0.30
	Very high (VH)	0.25 – 0.30 – 0.35
	Extra high (EH)	0.30 – 0.35 – 0.40
	Extra extra high (EEH)	0.35 – 0.40 – 0.45
Tool life (X5)	-	24 subsets (0 to 2280)

Table 4. *Training values for fuzzy logic and artificial neural networks in turning with high-speed steel (HSS) and tungsten carbide (WC) and reference roughness (R_{ref}), (Vc in m/min, DoC in mm, f_{tool} in mm, Tc in s, R_{ref} in µm).*

Tool	Vc	DoC	f_{tool}	Exp	Tc	%C	R_{ref}	Tool	Vc	DoC	f_{tool}	Exp	Tc	%C	R_{ref}
				02	108.4	0.1	1.74					01	62.22	0.1	1.96
				03	162.6	0.1	2.22					02	124.44	0.1	2.02
				04	202.6	0.15	3.02					03	186.66	0.1	1.22
				05	242.6	0.15	3.77					05	280.0	0.15	1.8
				06	282.6	0.15	1.87					06	326.67	0.15	0.98
				07	336.8	0.25	2.82					07	381.93	0.25	1.11
				09	445.2	0.25	3.04					09	492.45	0.25	1.58
				10	553.6	0.35	4.58					10	539.12	0.35	2.96
				11	662.0	0.35	5.40					11	585.79	0.35	3.74
HSS	40	0.5	0.2	13	824.6	0.1	2.28	WC	150	0.5	0.4	12	632.46	0.35	2.92
				14	878.8	0.1	1.96					13	694.68	0.1	1.92
				15	933.0	0.1	2.16					14	756.9	0.1	1.78
				16	973.0	0.15	1.69					16	865.79	0.15	1.72
				17	1013.0	0.15	2.56					17	912.46	0.15	1.6
				19	1107.2	0.25	1.8					18	959.13	0.15	1.24
				20	1161.4	0.25	3.66					19	1014.4	0.25	1.89
				21	1215.6	0.25	1.85					20	1069.7	0.25	1.2
				22	1324.0	0.35	4.66					21	1125.0	0.25	2.1
				23	1432.4	0.35	3.48					22	1171.6	0.35	2.89
				24	1540.8	0.35	4.72					23	1218.3	0.35	2.74

Table 5. *Training values for fuzzy logic and artificial neural networks in milling with high-speed steel (HSS) and tungsten carbide (WC) and reference roughness (R_{ref}), (Vc in m/min, DoC in mm, f_{tool} in mm, Tc in s, R_{ref} in µm).*

Tool	Vc	DoC	f_{tool}	Exp	Tc	%C	R_{ref}	Tool	Vc	DoC	f_{tool}	Exp	Tc	%C	R_{ref}
				01	94	0.1	2.27					01	95	0.1	0.61
				03	282	0.1	5.40					02	190	0.1	0.44
				04	376	0.15	2.98					03	285	0.1	0.44
				05	470	0.15	3.62					04	380	0.15	0.47
				06	564	0.15	3.94					05	475	0.15	0.46
				07	658	0.25	2.76					06	570	0.15	0.33
				09	846	0.25	4.28					07	665	0.25	0.46
				11	1034	0.35	2.28					08	760	0.25	0.21
				12	1128	0.35	2.9					09	885	0.25	0.55
HSS	40	0.5	0.15	13	1222	0.1	3.04	WC	150	0.5	0.15	11	1045	0.35	0.32
				14	1316	0.1	2.82					12	1140	0.35	0.68
				15	1410	0.1	1.61					13	1235	0.1	0.16
				17	1598	0.15	3.66					14	1330	0.1	0.38
				18	1692	0.15	1.86					16	1520	0.15	0.26
				19	1786	0.25	2.84					17	1615	0.15	0.29
				20	1880	0.25	2.15					19	1805	0.25	0.36
				21	1974	0.25	1.36					20	1900	0.25	0.24
				22	2068	0.35	2.15					22	2090	0.35	0.26
				23	2162	0.35	3.98					23	2185	0.35	0.38
				24	2256	0.35	3.42					24	2280	0.35	0.16

Since there were no ranges on the cutting conditions, the rules related to the fuzzy logic exercise were as follows:

Rules:

if X1 is VL and X2 is VL and X3 is VL and X4 is EL and X5 is T1 then Y is R1.

if X1 is VL and X2 is VL and X3 is VL and X4 is EL and X5 is T2 then Y is R2.

if X1 is VL and X2 is VL and X3 is VL and X4 is EL and X5 is T3 then Y is R3.

if X1 is VL and X2 is VL and X3 is VL and X4 is L and X5 is T4 then Y is R4.

…

if X1 is VL and X2 is VL and X3 is VL and X4 is EEH and X5 is T24 then Y is R24.

The Mamdani inference system was implemented for the fuzzy logic approach (figure 4).

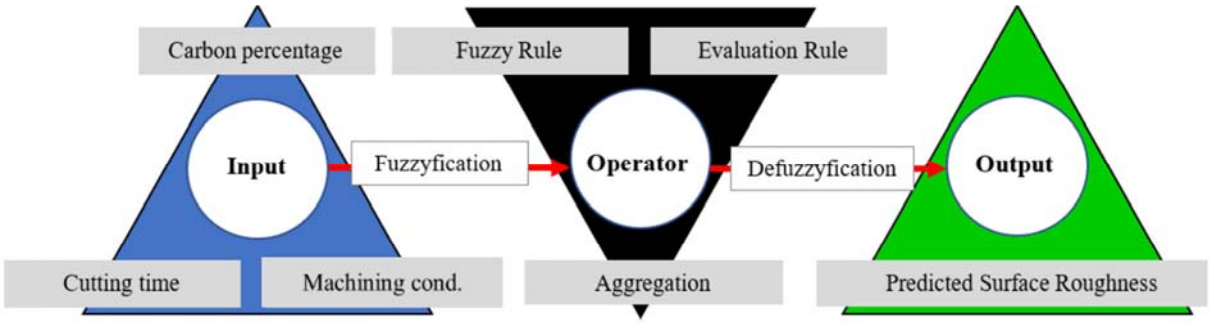

Figure 4. *Representation of the Mamdani Inference System in the works.*

The centroid of area was executed for the defuzzification of the predictive method.

The neural networks method was developed from the backpropagation of *Levenberg-Marquardt* to the Multi-Layers Perceptron (MLP) model. The architecture of the neural networks was 3-10-1 (figure 5). Ten (10) hidden layers helped to adjust the weight of the inputs to have interesting predicted values. For each prediction technique, twenty-four (24) experiences per tool and machining operation were implemented. Eighty (80) values for training and sixteen (16) to assess the system.

The performance of the system was weighed with the relative error ε and the Mean Square Errors (MSE) have been estimated with the predicted test and reference roughness values.

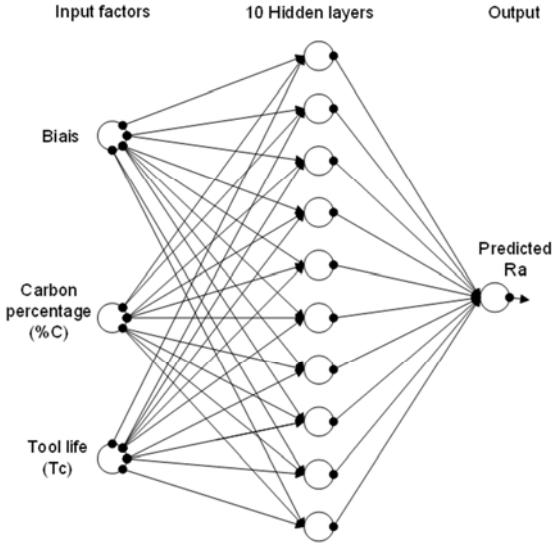

Figure 5. *Multi-layers' perceptron neural networks architecture.*

$$MSE=\frac{1}{N}\sum_{k=1}^{N}[R_p(k) - R_{ref}(k)]^2 \quad (2)$$

Where *Rp* is the Predicted roughness, *Rref* is the reference roughness or target roughness, and *N* is the number of data that helped for testing the algorithm [6].

3. Results and Discussion

3.1. Roughness Measurement

A total of ninety-six (96) hard surfaces were obtained from machining operations and were used to extract the reference roughness values and images. The set-up and the image acquisition protocol (figure 3) contributed to constitute a database of four hundred and eighty (480) color images with a spatial resolution of 640*480 pixels, with the radiometric resolution of 900KB, each image was associated to its roughness reference value.

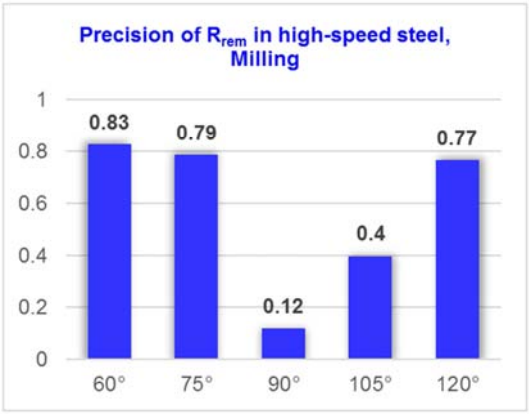

Figure 6. *Measurement precision of R_{rem} in high-speed steel in milling.*

The remote surface roughness precision (R_{rem}) of the first criterion (§2.3) related to the cutting tool, the milling

operation, and the acquisition angle is given in Figure 6. The acquisition angles of 60°, 75°, and 120° in milling portray a very interesting achievement of the method with precisions attaining 83%. The results revealed inappropriate acquisition angles in the interval [80°; 105°], no matter the machining operation. In turning, none of the angles disclosed precision above 50% (not presented here).

The results portrayed the angles of 60°, 75°, and 120° as interesting angles for machinists and metrologists for capturing images before processing. A large acceptable spread of angles can therefore guide to have interesting images, avoiding to enter the "dead valley" comprising [80° - 105°] where the results were not remarkable. A more interesting approach can include to the selection of region of interest (ROI) when processing the images. Definitely, the normal incidence 90° is revealed as not appropriate to extract image features. The results from the turning samples were not of a good conclusion (under 50% of precision) and have not been shown here.

Figure 7 portrays all-in-one precisions related to the first (blue and orange) and the second criteria (gray) explained in §2.3. It embodies the precision recorded with the high-speed steel (blue) and tungsten carbide (orange) with the milling operation.

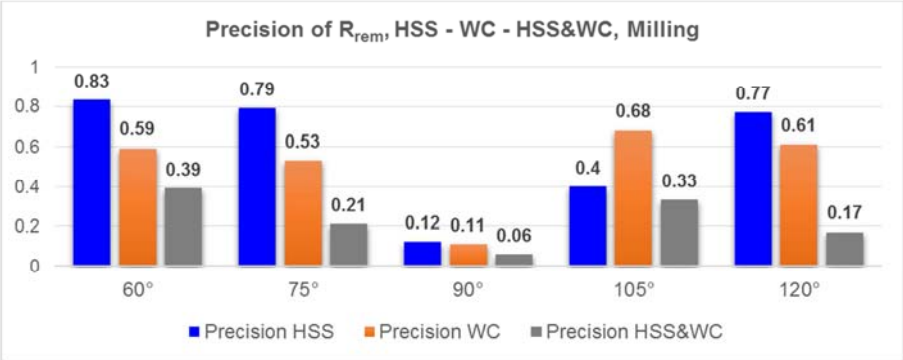

Figure 7. *Measurement Precisions of R_{rem} in High-Steel (HSS) and tungsten carbide (WC) in milling.*

The results laid out a surface roughness assessment tributary to cutting tools. Generally, in machining the best surface finish is achieved with the tungsten carbide tool giving the lowest reference roughness values, here it's observable that the high-speed steel tool adapts best to the method. This can be understood by the pronounced asperities on the high-speed steel machined surfaces which are presenting a clear-cut in surface illumination during the acquisition exercise. However, the poor unexpected precision of the second criterion helps to make a clear consideration of the cutting tool.

The distribution of values observed with the second criterion could be explained following three (03) major factors: the cutting conditions imposed by the cutting tools (difference in cutting speeds and feed), the surface production method, and the geometry of the tool point.

The overall results portrayed the most interesting acquisition angles at 60°, 75°, 105°, and 120°. The discordance of the precision tied up to the cutting tools, remains a major point of interest. Two (02) considerations can therefore be addressed: the measured specimens and the acquisition device and principle.

The specimens' final surface is a result of several elements. From the cutting tool perspective, it can be noticed from the results that there is a difference in precision within the same machining operation. An empirical approach here has set a better understanding of the impact of the tool geometry and points on the various steel grades together with heat diffusion and the laws of viscoplastic behavior [39]. In like manner, the results put back a nuance in the subdivision of the samples' surface finish in terms of stochasticity and determinism [40] but opens the scrutiny of input and machining phenomena [6].

Concerning the acquisition device, to solve the limitation imposed by the numerical aperture [9], the point-to-point acquisition protocol was implemented. By varying the angular position of the sensor around 90°, there was an improvement in equilibrating the surface feature illumination. This helped to strengthen the appreciation of the optical roughness results related to the acquisition angle. Furthermore, the existence of a discrepancy of the precision of the angles, even with the same tool, can be explained not only by the closeness to 90° of the acquisition angles, but also by the difference in the grades of the samples. This understanding underlines the impact of different mechanical and thermal induced experiences during machining operations and therefore serves as a practical demonstration of Keblouti *et al.'* works [41].

The 10x magnification of the acquisition device seemed to be weak to address the evaluation of optical roughness. The algorithm elaborated around the principle of the surface tester, enforced the correction of poor magnification. And so, the results of Kamguem et al., (2013) [13], by using 50x magnifications for the best correlation in assessing machined surface roughness, have been more elaborated with the use of lower magnification ranges.

Moreover, the findings in this remote monitoring of surface roughness approach display a practical illustration of ISO 4288:1996 about the total dependence of roughness parameters on machining operations and tools. And at the same time, they highlight the assertions of Nexhat et al. (2014) [42], Kanaa et al. (2016) [15] on controlling

roughness from the composition of the cutting tools and machined samples.

3.2. Surface Roughness Prediction

The precisions of the prediction of the average roughness (blue colour) with fuzzy logic (red colour) and neural networks (green colour) compared to the reference values are portrayed in Figure 8. The test values helped to appreciate the closeness of the reference to the prediction. And so, it can be observed that the fuzzy logic prediction stands as a good candidate for the close follow-up of the reference.

To conclude with accuracy about the deviation around the reference, table 6 was elaborated to assess the mean square errors between the reference values issued by the roughness tester and the test values from the prediction methods, considering the machining operations and the cutting tools. Table 7 has been laid to weigh the contribution of the carbon percentage (material content) in the precision of the prediction techniques regardless to the previous considerations.

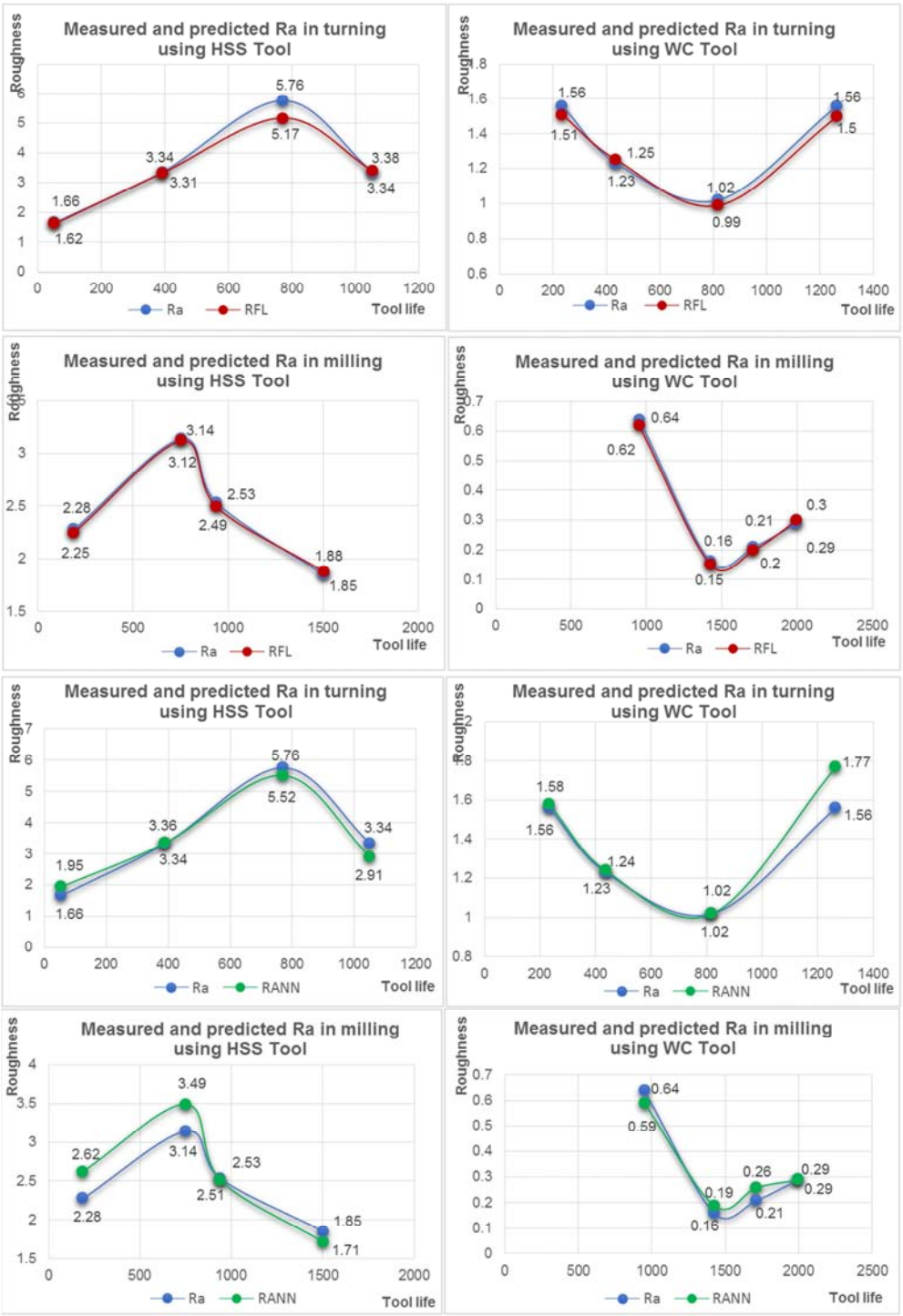

Figure 8. *Measured and predicted values of roughness in turning and milling operations using the HSS and WC tools.*

Table 6. *Mean square errors (MSE) for prediction with fuzzy logic and artificial neural networks with the consideration of machining operations and the cutting tools.*

		Run	%C	Fuzzy Logic (FL)			Artificial Networks (ANN)		
				R_a	R_{FL}	MSE	R_a	R_{ANN}	MSE
Turning	HSS	01	0.10	1.66	1.62	0.297	1.66	1.95	0.286
		02	0.15	3.34	3.38		3.34	2.91	
		01	0.25	3.34	3.31		3.34	3.36	
		01	0.35	5.76	5.17		5.76	5.52	
	WC	02	0.10	1.02	0.99	0.044	1.02	1.57	0.295
		01	0.15	1.56	1.5		1.56	1.77	
		01	0.25	1.23	1.25		1.23	1.24	
		02	0.35	1.56	1.51		1.56	1.58	
Milling	HSS	01	0.10	2.28	2.25	0.032	2.28	2.62	0.254
		02	0.15	1.85	1.88		1.85	1.71	
		01	0.25	3.14	3.12		3.14	3.49	
		01	0.35	2.53	2.49		2.53	2.51	
	WC	02	0.10	0.16	0.15	0.014	0.16	0.19	0.037
		02	0.15	0.21	0.20		0.21	0.26	
		02	0.25	0.29	0.30		0.29	0.29	
		01	0.35	0.64	0.62		0.64	0.59	

R_{FL}: Fuzzy Logic predicted Roughness - R_{ANN}: Artificial Neural Networks predicted Roughness.

The discrepancy observed in the mean square errors between the predicted values using fuzzy logic and neural networks (table 6) with the use of the high-speed steel and tungsten carbide tools, shows a minimum distance around the reference presenting a privileged choice of machining operation and cutting tool [28]. Fuzzy logic technique outperforms artificial neural networks in terms of the lowest mean square errors, giving force to the fuzzy logic supervised predictive method [28, 37].

Table 7. *Mean square errors (MSE) for prediction with fuzzy logic and artificial neural networks with the consideration of material content.*

%C	Fuzzy Logic (FL)			Artificial Neural Networks (ANN)		
	R_a	R_{FL}	MSE	R_a	R_{ANN}	MSE
0.10	1.66	1.62	0.000875	1.66	1.95	0.125775
	1.02	0.99		1.02	1.57	
	2.28	2.25		2.28	2.62	
	0.16	0.15		0.16	0.19	
0.15	3.34	3.38	0.00155	3.34	2.91	0.062775
	1.56	1.5		1.56	1.77	
	1.85	1.88		1.85	1.71	
	0.21	0.20		0.21	0.26	
0.25	3.34	3.31	0.00045	3.34	3.36	0.03075
	1.23	1.25		1.23	1.24	
	3.14	3.12		3.14	3.49	
	0.29	0.30		0.29	0.29	
0.35	5.76	5.17	0.08815	5.76	5.52	0.015225
	1.56	1.51		1.56	1.58	
	2.53	2.49		2.53	2.51	
	0.64	0.62		0.64	0.59	

R_{FL}: Fuzzy Logic predicted Roughness - R_{ANN}: Artificial Neural Networks predicted Roughness.

The mean square errors according to the material content show extremely low values, hence satisfying and even orienting the decision making in predicting with fuzzy logic using mild steels (0.10 to 0.25) to have maximum closeness to the reference values. The artificial neural networks, from tables 6 and 7, present a preference to medium steels, considering or regardless to machining operations, cutting tools, and material content.

The tool life, used as an input, refers to the wear of the cutting tool under normal operating conditions. The prediction results present the possibility of roughness control by the tool life [43] and reinforcing the assertions of Kanaa et al. (2016) [15] on the powerful impact of the tool life and the material content over the surface quality (finish) of the specimen.

The comparison of each predictive technique to reference roughness led to the juxtaposition of predictive precisions related to machining operations and cutting tools. The predictive precisions of average roughness (Ra) with fuzzy logic (red colour) and artificial neural networks (green colour) are portrayed in Figure 9.

Figure 9 (a) displays the precision in turning operation with tungsten carbide (WC) tool, with 97.06% and 90.19% for fuzzy logic and neural networks respectively. With the high-speed steel (HSS) tool, the precisions are 98.76% and 94.62% for fuzzy logic and neural networks, respectively.

Figure 9 (b) presents the precision in milling operation in tungsten carbide (WC) as 98.12% and 93.37% for fuzzy logic and neural networks, respectively. In high-speed steel (HSS), the precisions are 98.46% and 94.18% for fuzzy logic and neural networks, respectively.

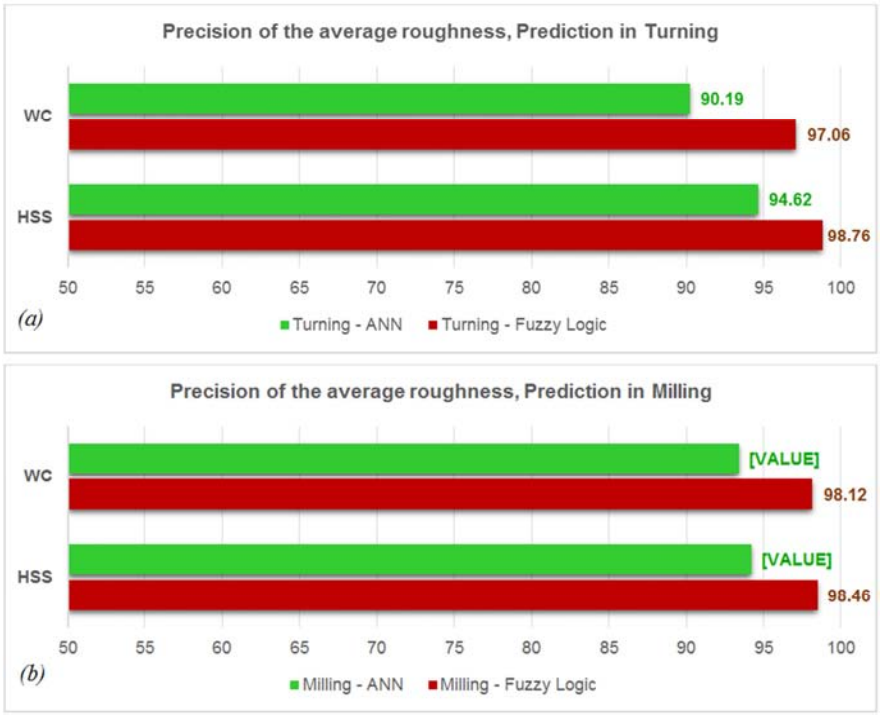

(a) Precision in turning – (b) precision in milling

Figure 9. *Prediction Precision of Ra in high-speed steel (HSS) and tungsten carbide (WC).*

All over the predictive techniques, the precision percentage is above 90. The robustness of the method is highlighted, all machining operations and cutting tools considered: the surface roughness can therefore be predicted with the tool life and samples' grades. This adds the list proposed by Vasanth et al. (2020) [30] of meaningful inputs in predicting machined surface roughness. In turning and milling operations, the tungsten carbide shows the lowest precisions and then establishes a preference to the high-speed steel for such exercise. The highest precisions are recorded in the milling operations.

4. Conclusion

The appropriate material selection, cutting tools, and cutting conditions are the major preoccupations of machinists and metrologists in surface roughness assessment and prediction. This paper presented a surface roughness remote measurement articulated on the acquisition angles of images and the prediction of surface finish based on the tool life and workpiece composition. The results portrayed:

(i) The effective possibility to achieve the non-contact measurement at 60°, 75°, and 120°, with precision attaining 83%.

(ii) The impact of the cutting tools on the surface finish. The high-speed steel tools demonstrated, all machining operations considered, the dominant precision in the models developed in this work.

(iii) The achievability of surface finish prediction with the tool life and workpiece content taken as input parameters. An overall precision above 90% is recorded for the fuzzy logic and neural networks predictive techniques.

(iv) The fuzzy logic predictive method surpasses, regardless of the cutting tools or the machining operations, the artificial neural networks.

At this level of surface metrology, this study opens the consideration of additional factors in executing the surface roughness remote monitoring. In like manner, there are trends of reviewing the reference measurement process of surface roughness to improve the remote monitoring precision.

Data Availability

The data used to support the findings of this study are available from the corresponding author upon request.

Conflicts of Interest

The authors declare that there is no conflict of interests regarding the publication of this paper.

References

[1] Goetz, M., *Les états de surface dans tous leurs états*. Micronora Informations – Revue du Salon International des microtechniques, N°114, Juillet 2008.

[2] Kalpakjian, S., and Schmid, S. *Manufacturing Processes for Engineering Materials*, 5th Edition, Pearson Education, inc. USA., 2008.

[3] Öztürk, B., & Fuat Kara (2020). *Calculation and Estimation of Surface Roughness and Energy Consumption in Milling of 6061 Alloy.* Hindawi. Advances in Materials Science and Engineering Volume 2020, Article ID 5687951, 12 pages, https://doi.org/10.1155/2020/5687951.

[4] Benardos, P. G., and Vosniakos G. C. (2002). *Predicting surface roughness in machining: a review.* International Journal of Machine Tools & Manufacture 43 (2003) 833–844; doi: 10.1016/S0890-6955(03)00059-2.

[5] Panda, A., Das, S. R., & Dhupal, D. (2017). *Surface Roughness Analysis for Economical Feasibility Study of Coated Ceramic Tool in Hard Turning Operation.* Process Integration and Optimization for Sustainability, 1 (4), 237–249. doi: 10.1007/s41660-017-0019-9.

[6] Juan, L., Xiaoping L., Steven L., Haibin O., Kai C., & Bing H. (2019). *An Effective ABC-SVM Approach for Surface Roughness Prediction in Manufacturing Processes*. Hindawi Complexity Volume 2019, Article ID 3094670, 13 pages, https://doi.org/10.1155/2019/3094670.

[7] Demange, M-L. Z. *La mesure de rugosité ? Quelques normes… et plusieurs dizaines de paramètres.* Magazine Mesures No 758, Octobre 2003. www.mesures.com.

[8] Anayet, U., Patwari, M. D., Arif, N. A., Chowdhury, S. I., & Chowdhury (2011). *3-D Contour Generation and Determination of Surface Roughness of Shaped and Horizontally Milled Plates Using Digital Image Processing.* International Journal of Engineering; Tome IX, Fascicule 3; ISSN 1584–2673.

[9] Leach, R. (2013). *Characterisation of Areal Surface Texture*. Springer-Verlag Heidelberg New York Dordrecht London; ISBN 978-3-642-36458-7 (eBook); Berlin, Germany; 355pgs.

[10] Stout, K., and Blunt, L. *Three-dimensional surface topography*. Kogan Page, London, England, 2000.

[11] Chand M., Aarti, M., Rina, S., Ojha, V. N., and Chaudhary, K. P. (2011). *Roughness measurement using optical profiler with self-reference laser and stylus instrument – A comparative study*. Indian Journal of Pure and Applied Physics, vol. 49, pp. 335-339.

[12] Liu, J., Lu, E., Huaian, Y., Menghui, W., Peng, A. (2017). *A new surface roughness measurement method based on a color distribution statistical matrix*. Measurement 103, pp. 165–178.

[13] Kamguem, R., Souheil, A. T., and Songmene, V. (2013). *Evaluation of Machined Part Surface Roughness using Image Texture Gradient Factor*. International Journal of Precision Engineering and Manufacturing, Vol. 14, No. 2, pp. 183-190.

[14] Koura, M. O., (2015). *Applicability of image processing for evaluation of surface roughness*. IOSR Journal of Engineering (IOSRJEN); Vol. 05, Issue 05 (May. 2015), ||V2|| pp. 01 – 08; ISSN (e): 2250-3021, ISSN (p): 2278-8719.

[15] Kanaa, T. F. N., Tchiotsop D., Fogue, M., Ngongang, L., Tsague, P. Y., & Njeugna, E. (2016). *Field and Image Based Assessment of the Tool's Lifespan Impact on Roughness Parameters in a Context of Advanced Machine Depreciation*. Engineering and Technology. Vol. 3, No. 1, pp. 12-18.

[16] Manjunatha, R., Rajashekar, B. M., Rajaprakash, N. S., Mohan, G. (2017). *Evaluation of Surface Roughness of Machined Components using Machine Vision Technique.* International Journal of Engineering Development and Research (IJEDR), IJEDR1704203, Vol. 5, Issue 4, ISSN: 2321-9939.

[17] Szydlowski, M., Powalka, B., & Marchelek K. (2010). *Digital Image Processing in Surface Quality Inspection*. Proceedings of the ASME 2010 10th Biennial Conference on Engineering Systems Design and Analysis (ESDA 2010); July 12-14, 2010, Istanbul, Turkey.

[18] Huaian, Y. I., Jian, L. I. U., Enhui L. U., & Peng A. O. (2016). *Measuring grinding surface roughness based on the sharpness evaluation of colour images*. Measurement Science and Technology; Meas. Sci. Technol. 27 (2016) 025404 (14pp); IOP Publishing; doi: 10.1088/0957-0233/27/2/025404.

[19] Suhail, S. I. M., Mahashar, J. A., Siddhi, J. H., and Murugan, M. (2018). *Vision based system for surface roughness characterisation of milled surfaces using speckle line images*. 2nd International Conference on Advances in Mechanical Engineering (ICAME 2018); IOP Conf. Series: Materials Science and Engineering 402 (2018) 012054; doi: 10.1088/1757-899X/402/1/012054.

[20] Mateos, S., Valiño, G., Zapico, P., Fernández P., & Rico J. C. (2014). Non-Contact Measurement of Surface Roughness by Conoscopic Holography Systems. Proceedings of the World Congress on Engineering 2014 Vol II, WCE 2014, July 2 - 4, 2014, London, United Kingdom.

[21] Grzegorz, F. (2010). *Modelling of Fuzzy Logic Control System Using the Matlab Simulink Program*. Technical Transactions, Mechanics, Issue 8, vol. 107, pp. 73-81.

[22] Kuram, E., and Ozcelik, B. (2013). *Fuzzy logic and regression modelling of cutting parameters in drilling using vegetable based cutting fluids*. Indian Journal of Engineering & Materials Sciences. Vol. 20, pp. 51-58.

[23] Kovac, P., Rodic, D., Pucovsky, V., Savkovic, B., & Gostimirovic, M. (2013). *Application of fuzzy logic and regression analysis for modeling surface roughness in face milliing.* J Intell Manuf (2013) 24: 755–762. DOI 10.1007/s10845-012-0623-z.

[24] Abhinav, S., Shrivastava, D., & Harsh, P. (2015). *Predict the Surface Finish by using Fuzzy Logic Techniques in ECM Processes*. International Research Journal of Engineering and Technology (IRJET), Vol. 2 Issue 3, pp. 2118-2121.

[25] Barzani, M. M., Zalnezhad, E., Sarhan, A. A. D., Farahany, S., & Ramesh, S. (2015). *Fuzzy Logic Based Model for Predicting Surface Roughness of Machined Al-Si-Cu-Fe Die Casting Alloy Using Different Additives-Turning*. Measurement, doi: http://dx.doi.org/10.1016/j.measurement.2014.10.003.

[26] Tzu-Liang, T., Udayvarun, K., & Yongjin, K. (2016). *A novel approach to predict surface roughness in machining operations using fuzzy set theory.* Journal of Computational Design and Engineering Vol. 3; pp1–13.

[27] Vishal, S. S., Suresh, D., Rakesh, S., & Sharma, S. K. (2008); *Estimation of cutting forces and surface roughness for hard turning using neural networks.* J Intell Manuf. DOI 10.1007/s10845-008-0097-1.

[28] Vrabel, M., Mankovaa, I., Benoa, J. J., & Tuharský (2012). *Surface roughness prediction using artificial neural networks when drilling Udimet 720*. Procedia Engineering 48 (2012) pp. 693–700.

[29] Ramesh, S., Karunamoorthy, L., Palanikumar, K. (2012). *Measurement and analysis of surface roughness in turning of aerospace titanium alloy (gr5)*. Measurement, vol. 45, pp. 1266–1276, doi: 10.1016/j.measurement.2012.01.010.

[30] Vasanth, X., Ajay, P., Paul S., Varadarajan, A. S. (2020). *A neural network model to predict surface roughness during turning of hardened SS410*. Steel Int. J. Syst. Assur. Eng. Manag. https://doi.org/10.1007/s13198–020-00986-9.

[31] Akkus, H., and Asilturk, I., (2011). *Predicting Surface Roughness of AISI 4140 Steel in Hard Turning Process through Artificial Neural Network, Fuzzy Logic and Regression Models*. Scientific Research and Essays, Vol. 6 Issue 13, pp. 2729-2736.

[32] Sekulic, M., Pejic, V., Brezocnik, M., Gostimirović, M., & Hadzistevic, M. (2018). *Prediction of surface roughness in the ball-end milling process using response surface methodology, genetic algorithms, and grey wolf optimizer algorithm.* Advances in Production Engineering & Management; Vol. 13, Number 1, ISSN 1854–6250, pp 18–30.

[33] Al-Zubaidi, S., Jaharah, A. G., & Che, H. (2013). *Prediction of Surface Roughness When End Milling Ti6Al4V Alloy Using Adaptive Neuro-fuzzy Inference System*. Hindawi Pub. Corp., Modelling and Simulation in Engineering, Article ID932094, 12 pages.

[34] Kuldip, S. S., Sachin, S., & Kant, G. (2015). *Optimization of Machining Parameters to Minimize Surface Roughness using Integrated ANN-GA Approach*. The 22nd CIRP conference on Life Cycle Engineering, Procedia CIRP 29, pp. 305-310.

[35] Çaydas, U., and Ekici, S. (2010). *Support vector machines models for surface roughness prediction in CNC turning of AISI 304 austenitic stainless steel*. J Intell Manuf. DOI 10.1007/s10845-010-0415-2.

[36] Ngerntong, S., and Butdee, S. (2020). Surface roughness prediction with chip morphology using fuzzy logic on milling machine, Materials Today: Proceedings, https://doi.org/10.1016/j.matpr.2020.02.506.

[37] Kanisha, T. C., Kuppanb, P., Narayananc, S., & Ashokd, S. D. (2014). A Fuzzy Logic based Model to predict the improvement in surface roughness in Magnetic Field Assisted Abrasive Finishing. 12th Global Congress on Manufacturing and Management, GCMM 2014, Procedia Engineering 97 (2014) 1948–1956.

[38] Rajesh, M., and Manu, R. (2014). *Prediction of surface roughness of freeform surfaces using Artificial Neural Network.* 5th International & 26th All India Manufacturing Technology, Design and Research Conference (AIMTDR 2014) December 12th–14th, 2014, IIT Guwahati, Assam, India.

[39] Seifi, R., Abbasi, K., & Asayesh, M. (2017). *Effects of Contact Surface Roughness of Interference Shaft/Bush Joints on its Characteristics. Iranian Journal of Science and Technology, Transactions of Mechanical Engineering, 42 (3), 279–292.* doi: 10.1007/s40997-017-0082-4.

[40] Dietrich, R., Garsaud, D., Gentillon, S., & Nicolas, M. (2005). *Précis de Méthodes d'usinage, Méthodologie, Production et Normalisation*. AFNOR Nathan, Paris.

[41] Keblouti, O., Boulanouar, L., Bouziane, R., & Azizi, M. W. (2017). *Impact du revêtement et des conditions de coupe sur le comportement à l'usure des outils et sur la rugosité de la surface usinée*, U. P. B. Sci. Bull., Series D, Vol. 79, Issue 3, ISSN 1454-2358.

[42] Nexhat, Q., Jakupi, K., Bunjaku, A., Bruçi, M., & Osmani, H. (2014); *Effect of Machining Parameters and Machining Time on Surface Roughness in Dry Turning Process*. 25th DAAAM International Symposium on Intelligent Manufacturing and Automation, DAAAM 2014, Procedia Engineering 100, (2015) 135–140.

[43] Pimenov, D. Y., Bustillo, A., & Mikolajczyk, T. (2018). *Artificial intelligence for automatic prediction of required surface roughness by monitoring wear on face mill teeth*. Journal of Intelligent Manufacturing (2018) 29: 1045–1061. https://doi.org/10.1007/s10845-017-1381-8.